ALLPLAN
A NEMETSCHEK COMPANY

Received: 8 July 2020 | Revised: 4 October 2020 | Accepted: 22 October 2020

DOI: 10.1002/suco.202000415

TECHNICAL PAPER

fib CEB-FIP WILEY

Delamination detection on a concrete bridge deck using impact echo scanning

Johannes F. Scherr | **Christian U. Grosse**

Chair of Non-Destructive Testing, Technical University of Munich, Munich, Germany

Correspondence
Johannes F. Scherr, Chair of Non-Destructive Testing, Technical University of Munich, Franz-Langinger-Straße 10, 81245 Munich, Germany.
Email: j.scherr@tum.de or zfp@cbm.bgu.tum.de

Funding information
Allianz Industrie Forschung; Niedersächsisches Landesbehörde für Straßenbau und Verkehr

Abstract

In this large-scale field study we use a prototype impact-echo scanner to detect delaminations on a concrete bridge deck surveying in total over 17,000 m^2. Delaminated bridge sections are known from manual sounding and coring. A large-scale damage assessment is necessary to identify the need of repair work. Based on first results, two lanes of the bridge are repaired and in subsequent tests the bonding of fresh and old concrete is examined. It shows that delaminations found on the bridge deck surface are unevenly distributed with more defects on the southbound lanes. This indicates constructional problems during the concrete placement. The developed scanner excites stress waves by dropping steel solenoids on the surface and recording the impact-echo frequency by air-coupled microphone arrays. It is pushed at a speed of 600 m/h, hitting the surface 300 times per square meter. The recorded data is preprocessed on site with an automated delamination detection threshold implemented. Found delaminations are transferred to a bridge map to allow an overall damage assessment.

KEYWORDS

concrete bridge deck, delamination, impact echo, lamb waves

1 | INTRODUCTION

The 1,460 m-long bridge Moorbrücke carries the federal freeway 27 in Bremerhaven in Northern Germany over marshland. In the coastal region, the concrete bridge deteriorated since its construction in 1970 with multiple locations of delaminated slabs detected by manual sounding and coring. The bridge is classified as" not fit for the future" and will therefore be replaced in the upcoming 10–20 years. Until then the bridge and its load carrying capacity must be sustained for logistical and safety reasons. The overall damage needs to be assessed by non-destructive testing (NDT) techniques in an efficient and reliable way. The local road authority tested several NDT techniques including ultrasound, manual sounding and infrared thermography but failed to assess the damage on a large scale. The bridge carries six lanes consisting of two lanes and one breakdown lane in each direction. Both the northbound and southbound lanes are mounted on separate superstructures. In longitudinal direction, the bridge is segmented in 14 subfields of each 104 m

Discussion on this paper must be submitted within two months of the print publication. The discussion will then be published in print, along with the authors' closure, if any, approximately nine months after the print publication.

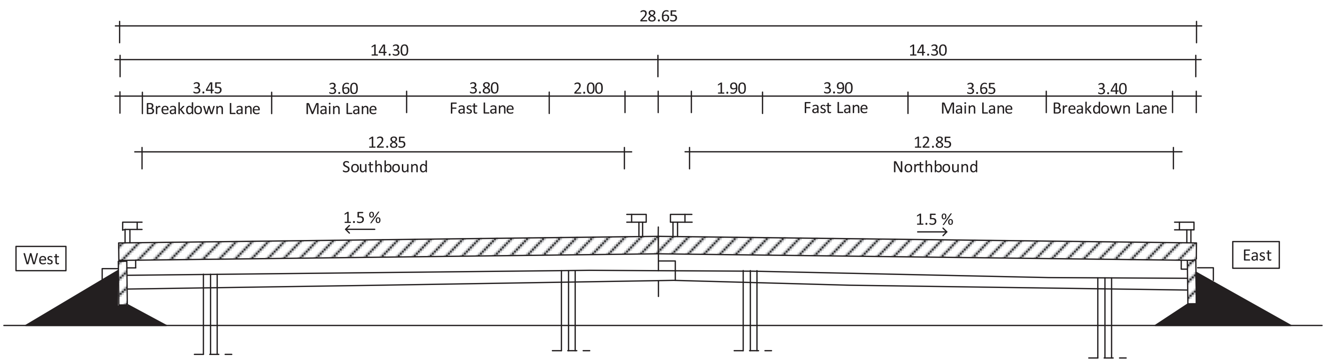

FIGURE 1 East-west cross section of the Moorbrücke. All values are given in metres

length which are connected by expansion joints. The bridge is supported by crossbars in 6.30 m intervals. It is oriented in North–South direction and spans an area of 65,000 m^2 of which around 24,000 m^2 are trafficked road surface. The bridge deck is built of 33 cm reinforced gravel concrete and a 7 cm wearing layer of crushed aggregate concrete on top which contains the upper most rebar layer. The concrete bridge deck is directly driven on a road surface in a modern sense does not exist. The design of the bridge corresponds to the specifications of DIN 1075 (1955-04-00) "Heavy Bridges - Calculation", Section 4.2 "Directly Trafficked Reinforced Concrete Carriageway Slabs without Particular Sealing" and represents a normatively regulated construction method at the time of planning and construction.[1] The bridge is founded on concreted end-bearing steel piles to transfer the loads of the bridge through the weak strata of the swamp. The heads of the piles tie into the 80 cm high and 50 cm wide crossbars which are monolithically connected to the bridge deck. The bridge construction is thus seen as a 40 cm thick plate with infinite lateral extent. Figure 1 shows an east–west cross section of the bridge. The coring found delaminations in between the two concrete layers which are believed to originate from a cold joint during the wet-on-wet concreting in the construction phase of the bridge.

1.1 | NDT and impact echo

The Impact echo (IE) method was developed in the 1980's by the National Institute of Standards and Technology and Cornell University as a non-destructive testing technique for plate-like concrete structures.[2] Since then IE has proven applicable in numerous situations including defect localization, thickness measurement of slabs and material characterization.[3–6] It is an elastic wave method that examines the transient vibrational response of a plate-like structure to a mechanical impact.[7] The underlying Lamb wave theory defines a laterally infinite plate by three independent parameters: shear wave speed, Poisson's ratio and thickness.[8] A transient impact generates a reverberating resonance exhibiting coupled longitudinal and transverse motion that are divided in symmetric (S) and anti-symmetric (A) modes. The zero group velocity (ZGV) point of the first order symmetric (S1) Lamb modes dispersion curve corresponds to the so called IE frequency.[9] With known P-wave velocity the IE frequency can be related empirically to the plate thickness by

$$h = \frac{\beta v_p}{2 f_{IE}}, \tag{1}$$

where h is the plate thickness and β a correction factor that depends on Poisson's ratio of the material (0.945 to 0.957 for concrete[9]); v_p denotes the P-wave velocity and f_{IE} the IE frequency. The formula can be used inversely to calculate the IE frequency with known plate thickness and P-wave velocity. The calculation of the plate thickness is often underestimated due to incorrect assumptions of Poisson's ratio.[10] For the presented case study, such deviations are considered negligible because we focus on the detection of delaminations not on measurements of the plate thickness. The vibrational response of the plate is analyzed in the frequency spectrum where a maximum peak at the IE frequency is visible in an undisturbed plate.[11] In a delaminated plate, dependent on the depth of the defect, low frequent flexural vibrations representing the out-of-plane vibration of the delaminated part dominate the frequency spectrum and indicate damages.[7,11] The measured frequency relates to the depth of the defect where low frequent flexural vibrations indicate shallow defects and frequencies higher than the IE frequency indicate deep-lying defects.[12] The minimum detectable size of a delamination is defined by the width-to-depth ratio whereas the width of the delamination should be five times larger than the defect depth.[13] An inspector can typically hear the difference between an intact and a delaminated plate when both the IE frequency and flexural vibration are in the human hearing range. To resolve the problem of this subjective impression, surface bound accelerators and microphones can be deployed to record the signal. For small surveys, this might be sufficient but for large bridge decks automated stress pulse excitation and non-contact receivers are needed.

1.2 | Existing technology

Numerous impact echo scanning devices have been presented in the past years that allow a rapid bridge deck assessment. All of them rely on a mechanical impact on the concrete surface while the receivers are either air coupled microphones or surface attached accelerometers. Gucunski developed a moving robotic platform incorporating four non-destructive evaluation techniques namely, impact echo, GPR, electrical resistivity and ultrasonic surface waves along with optical cameras. The device measures up to 1,000 m^2 of bridge deck per hour.[14] Mazzeo invented an impact echo device using rolling chain mats which are mounted on wheels mounted on a hinged trailer. Its speed ranges from 10 km/h to 55 km/h which makes it the fastest available device.[15] An impact echo device by Guthrie uses a steel mallet along with an air coupled microphone in a scanning fashion.[16] Zhu showed how air coupled sensors eliminate the need for mechanical coupling and further described the suitability of micro-electro-mechanical system (MEMS) microphones for NDT of concrete[12].[17] Other devices are constructed by Tinkey,[18] Zhang[19] or Sun.[20]

2 | IMPACT ECHO SCANNING DEVICE

The impact echo scanning device developed consists of three impactor and recording units, a signal processing unit, a Real Time Kinematic Global Positioning System (RTK-GPS) and a movable platform on which the units are mounted. The impactor and receiver units are each equipped with three steel solenoid impactors and a 30 cm diameter (0.07 m^2) microphone array comprising 35 micro-electro-mechanical system (MEMS) microphones. The impactors are steel ball dropping solenoids with an internal shock sensor that initializes the signal recording. Multiple, unwanted bouncing of the impactor on the concrete surface is prevented by lifting the steel

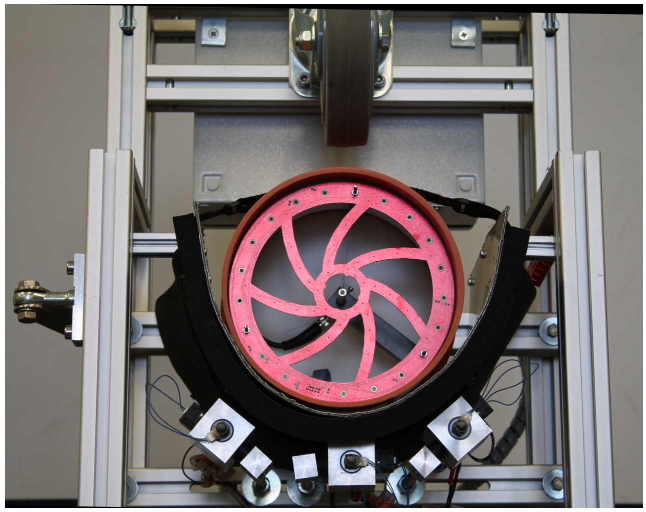

FIGURE 2 Bottom view of impactor and recording unit showing the three steel solenoids and the MEMS microphone array

solenoids shortly after the impact. Multiple bouncing must be avoided to obtain an unambiguous signal. The impact rate of the solenoids is tied to the speed of the device with a maximum speed of 600 m/h. The emitted IE frequency is recorded by the microphone array whose shape (Figure 2) assures the greatest sensitivity to the emitted wave perpendicular to the concrete surface and damps lateral traffic noise.[21] The recording time of the microphone array is 12.5 ms after each impact. The distance from impact position to the outer rim of the microphone array is 3.5 cm. To reduce ambient noise a foam is mounted around the array for acoustical insulation. A surveyor's wheel measures the scanning distance. The construction design of the 1.80 m wide device leaves a 60 cm gap in between each of the three modules. The scanner covers an area of 0.9 m^2 per meter pushed and 540 m^2 per hour. To cover the whole width the scanner must be displaced by 30 cm after each measurement run. Since the IE frequency is exhibited only in the area around the impact position each module only records its own emitted signal. The size of a detected delamination is assumed to be the size of the microphone array thus 0.07 m^2. Figure 3 shows a frontal view of the device as it is pushed on the road.

2.1 | Data processing

After every impact the emitted pressure wave is recorded at each of the 35 MEMS Microphones. To increase the signal to noise ratio (SNR) the 35 signals are stacked. A fast Fourier transformation (FFT) is executed to analyze the dominant peaks in the spectrum. Bandpass filtering is applied to include the presumed IE frequency and

FIGURE 3 Frontal view of the scanner showing the three impact and recording units, the data processing unit with laptop and the rolling cart as it is pushed on the road

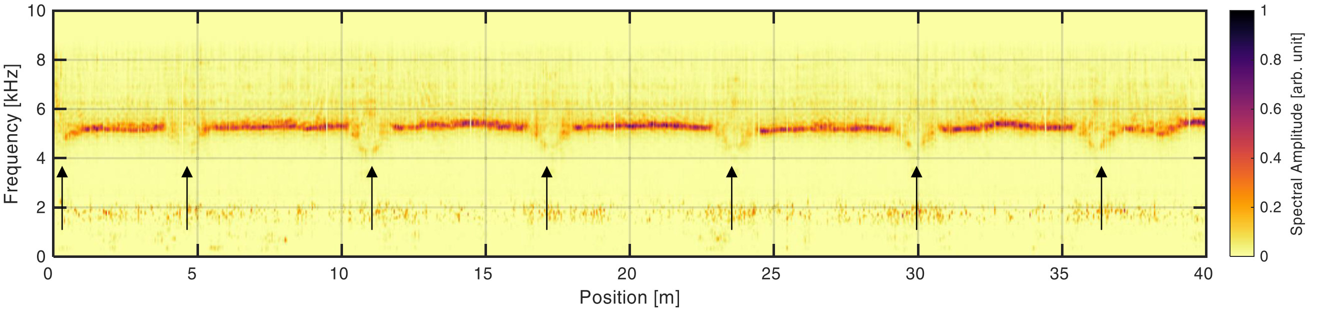

FIGURE 4 Distance-frequency plot of subfield with intact plate structure. The IE frequency can be seen at 4.9-5.1 kHz with interruptions every 6.30 m due to supporting crossbars. The continuous frequency band in between the crossbars indicates an intact plate without delaminations. Arrows indicate the positions of the crossbars

flexural vibration frequencies and to exclude noise. The data is displayed as distance-frequency plots showing the IE frequency and its deviations. Each recorded trace is tagged with a GPS mark and waypoint to achieve accurate positioning. An automated delamination detection is implemented in the code in a way that a delamination is indicated when the IE frequency is absent and a flexural vibration is visible at the same location. At the location of the crossbars where no IE frequency can form it is sufficient that a flexural vibration is present in the data.

3 | FIELD STUDY AND RESULTS

Three surveys were carried out on the Moorbrücke in May 2017, April 2019 and October 2019 assessing approximately 17,600 m^2 of concrete bridge deck surface. On all dates, the lanes to be measured were closed because of ongoing construction work. The IE frequency of the bridge is measured at 4900 Hz-5,100 Hz and with known plate thickness of 40 cm the P-wave velocity can be calculated by the formula in Section 1.1 to 4,083 m/s to 4,250 m/s. The scanner was pushed at a speed of 500 m/h making approximately 300 impacts per square meter with the nine solenoids. The data was stored on the mounted laptop and partially processed during the measurements. Figure 4 shows a 45 m distance-frequency plot of a measurement on a subfield. At the position of the supporting crossbars the plate structure is interrupted which inhibits the formation of lamb waves hence no IE frequency is visible.

Figure 5 shows a distance-frequency plot of a bridge subfield with found delaminations. The IE frequency band is interrupted at several locations and flexural vibrations are indicated by high amplitudes at low frequencies.

In May 2017 approximately 2,200 m^2 of the southbound lanes were surveyed with 689 delaminations found corresponding to approximately 48 m^2 or 2 % of the surveyed area. Concrete cores were taken which verified the results from the impact echo measurements. Based on the results the local road authority decided to repair the

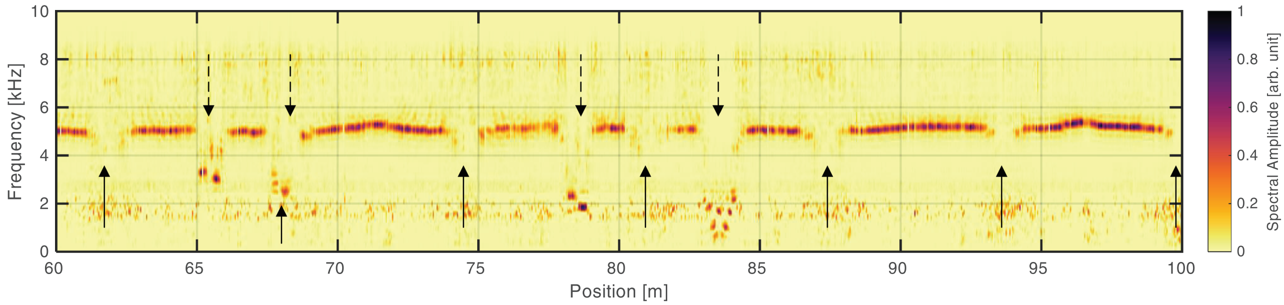

FIGURE 5 Distance-frequency plot of subfield with delaminations. The IE frequency is visible at 4.9-5.1 kHz with interruptions every 6.30 m due to supporting crossbars. The interrupted frequency band at 65-66 m, 67 m, 78 m and 83-84 m with higher amplitudes at lower frequencies indicates a delaminated plate structure. Solid arrows indicate the positions of the crossbars. Dashed arrows indicate the position of the delaminations

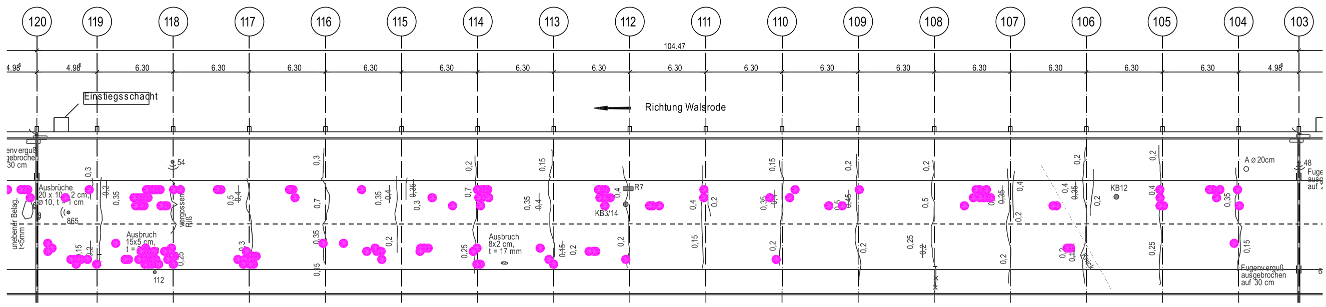

FIGURE 6 Delaminations on the southbound lanes displayed as pink dots in a CAD-file from the May 2017 survey. Here, both lanes are still in unrepaired condition

southbound main lane. In the repair the uppermost 10–15 cm of old concrete were blast-off with a water jet and fresh concrete was anchored with around 70,000 steel anchors to the underlying gravel concrete.

In the second survey in April 2019, one aim was to assess the quality of the repair by verifying the bonding of new and old concrete on the southbound main lane. Apart from that, selected subfields of the northbound lanes were surveyed to find delaminations. The bonding of fresh and old concrete is considered a success given that the repaired concrete plate exhibits the same IE frequency as prior to the repair. On the repaired southbound main lane an area of 2,600 m^2 was surveyed and 69 delaminations were found corresponding to 4.8 m^2 or 0.18 % of the surveyed area. Based on these results the road authority concluded that the repair of the lane was successful.

In September 2019, the southbound fast lane was repaired now having both southbound lanes bearing a new bridge deck surface. The third study in October 2019 surveyed 2,600 m^2 of the previously repaired southbound fast lane and 8,576 m^2 of the northbound lanes. The repaired southbound fast lane showed 43 delaminations corresponding to 3 m^2 or 0.12 % of the surveyed area indicating a successful repair. The northbound main lane showed 51 delaminations corresponding to 3.6 m^2 or 0.09 % of the surveyed area while the northbound fast lane showed 80 delaminations corresponding to 5.6 m^2 or 0.12 % of the surveyed area.

In a final step, all delaminations are imported in a CAD-file of the bridge to allow an overall damage evaluation. The overall damage assessment shows that IE scanning revealed that most delaminations can be found on the two southbound lanes. The repair was able to succesfully reduce the delaminations. The two northbound lanes do not show large numbers of delaminations. The scanner was pushed 20 km in total requiring around 50 man-hours divided in 8 days. Figures 6 and 7 show the damage evolution with delaminations shown as pink dots prior to and after repair, respectively. Table 1 lists the measured areas and related delaminations.

4 | DISCUSSION

Size and depth of delaminations are difficult to quantify in impact echo measurements. In the present case only

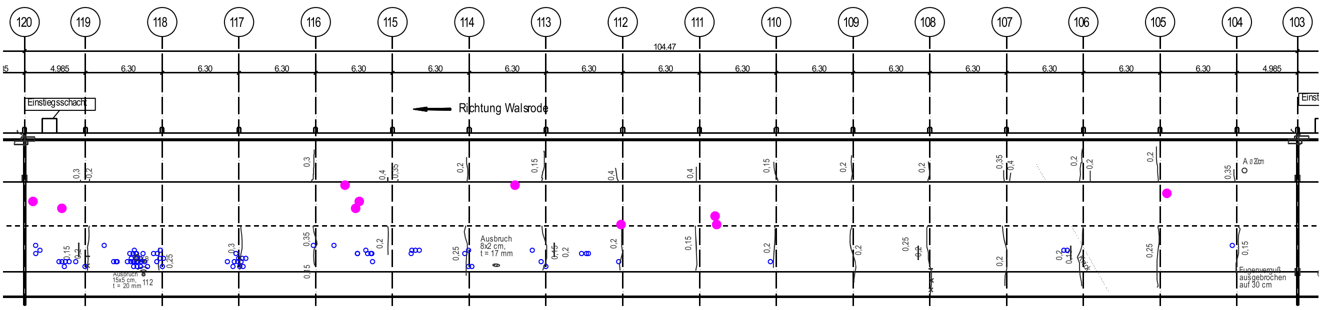

FIGURE 7 Delaminations on the southbound lanes displayed as pink dots in a CAD-file from the October 2019 survey. It can be seen that only few delaminations are detected after the repair of the two southbound lanes which indicates a successful repair

TABLE 1 Results of the three surveys. *Including the delaminations of the April 2019 survey

Survey date	Lane	Surveyed area [m^2]	Delaminations	Delaminated area [m^2]	Delaminated area [%]
May 2017	Southbound main	703	218	15	2.1
	Southbound fast	1,497	471	33	1.9
April 2019	Southbound main	2,600	69	4.8	0.18
	Northbound main	404	12	0.84	0.02
	Northbound fast	1,216	40	2.8	0.02
October 2019	Southbound fast	2,600	43	3	0.12
	Northbound main	3,900	51*	3.6	0.09
	Northbound fast	4,676	80*	5.6	0.12

flexural vibration frequencies lower than the IE frequency are found in the data suggesting shallow defects. The assumption that the size of delamination is equal to the size of the microphone array is made because the stacking of each recorded trace averages the signal over the size of the array. It is therefore possible to overestimate the size of defects smaller than the array size. A dense testing grid thus can avoid an underestimation of defect size. In this field study, the road authority was rather interested in a large-scale damage overview than the precise location of each single delamination. The spatial resolution is considered to be sufficient. With a scanning capability of 540 m^2/h the device is considerably faster than manual sounding however it is too slow to be used in running traffic.

5 | CONCLUSION

The primary aim of this study, the large-scale damage assessment by detection of delaminations on the Moorbrücke was accomplished fast and reliable. Coring verified the found delaminations by impact echo scanning. The secondary aim, the assessment of the bonding of fresh and old concrete and thus the proof of successful repair work was successfully verified by measuring the same IE frequency before and after repair. All measurements took place with running traffic nearby but noise was successfully suppressed by the receiver design. The measured bridge lanes show significant differences in damage what supports the idea of a cold joint during concreting on the southbound main lane. Based on the impact echo measurements cost intensive decisions to repair the southbound lanes were made. This shows the reliability of the method and acquired data.

ACKNOWLEDGMENTS

Supported by TUM International Graduate School of Science and Engineering (IGSSE). The authors are thankful for the valuable contributions of Sebastian Münchmeyer (electrical engineer at the Institute) who helped performe the measurements and Robin Groschup who performed the groundwork for this project. This work was funded by the funding program “Central Innovation Programme for small and medium-sized enterprises (SMEs)” of the Federal Ministry for Economic Affairs and Energy in Germany as well as the Lower Saxony State Authority for Road Construction and Traffic.

CONFLICTS OF INTEREST

The authors declare no conflict of interest.

AUTHOR'S CONTRIBUTIONS

Johannes Scherr wrote the article, performed the measurements and processed the data. Christian Grosse supervised the work and helped edit the article.

DATA AVAILABILITY STATEMENT

The data that support the findings of this study are available from the corresponding author upon reasonable request.

ORCID

Johannes F. Scherr https://orcid.org/0000-0003-1598-6223

REFERENCES

1. DIN German Institute for Standardization. DIN 1075 (1955-04-00) Heavy Bridges - Calculation: Betonbrücken - Bemessung Und Ausführung. Beuth Verlag GmbH. 1955-04-00; 93.040. Published 1955-04-00
2. Sansalone MJ, Carino NJ. Impact Echo: A Method for Flaw Detection in Concrete Using Transient Stress Waves. NBSIR 86–3452, National Bureau of Standards 1986.
3. Cheng C, Sansalone M. The impact-echo response of concrete plates containing delaminations: Numerical, experimental and field studies. Mater. Struct. 1993;26(5):274–285.
4. Sansalone MJ, Streett WB. Impact-Echo. Nondestructive evaluation of concrete and masonry. Jersey Shore, PA: Bullbrier Press, 1997.
5. Tofeldt O. Lamb wave evaluation of concrete plates, [Dissertation]. Lund University; 2017.
6. Grosse CU, Ohtsu M. Acoustic emission testing. Berlin Heidelberg: Springer-Verlag, 2008.
7. Kee S-H, Gucunski N. Interpretation of flexural vibration modes from impact-echo testing. J. Infrastruct. Sys. 2016;22(3): 4016009. https://doi.org/10.1061/(ASCE)IS.1943-555X.0000291.
8. Auld BA. Acoustic fields and waves in solids. Florida: Krieger Publishing, 1990.
9. Gibson A, Popovics JS. Lamb wave basis for impact-echo method analysis. J Eng Mech. 2005;131(4):438–443. https://doi.org/10.1061/(ASCE)0733-9399(2005)131:4(438).
10. Baggens O, Rydén N. Systematic errors in impact-Echo thickness estimation due to near field effects. NDT & E Int. 2015;69: 16–27. https://doi.org/10.1016/j.ndteint.2014.09.003.
11. Zhu J, Popovics JS. Imaging concrete structures using air-coupled impact-echo. J Eng Mech. 2007;133(6):628–640. https://doi.org/10.1061/(ASCE)0733-9399(2007)133:6(628).
12. Zhu J, Popovics JS. Non-contact imaging for surface-opening cracks in concrete with air-coupled sensors. Mater. Struct. 2005;38(9):801–806. https://doi.org/10.1007/bf02481652.
13. Oh T, Popovics JS, Sim S-H. Analysis of vibration for regions above rectangular delamination defects in solids. J Sound Vib. 2013;332(7):1766–1776. https://doi.org/10.1016/j.jsv.2012.11.003.
14. Gucunski N, Maher A, Ghasemi H. Condition assessment of concrete bridge decks using a fully autonomous robotic NDE platform. Bridge Struct. 2013;9(2, 3):123–130. https://doi.org/10.3233/BRS-130058.
15. Mazzeo BA, Guthrie WS. Algorithms for highway-speed acoustic impact-echo evaluation of concrete bridge decks. AIP Conf. Proc. 2018;1949(1):30010. https://doi.org/10.1063/1.5031533.
16. Guthrie WS, Larsen JL, Baxter JS, Mazzeo BA. Automated air-coupled impact-Echo testing of a concrete bridge deck from a continuously moving platform. J. Nondestructive Evaluation. 2019;38(1):32. https://doi.org/10.1007/s10921-019-0566-9.
17. Ham S, Popovics JS. Application of micro-electro-mechanical sensors contactless NDT of concrete structures. Sensors. 2015; 15(4):9078–9096.
18. Tinkey Y, Olson LD, Miller PK, Tanner JE. Vehicle-Mounted Bridge Deck Scanner: Final Report for Highway IDEA Project 132. Accessed, April 20 2020. http://onlinepubs.trb.org/onlinepubs/idea/finalreports/highway/NCHRP132_Final_Report.pdf
19. Zhang G, Harichandran RS, Ramuhalli P. An automatic impact-based delamination detection system for concrete bridge decks. NDT & E Int. 2012;45(1):120–127. https://doi.org/10.1016/j.ndteint.2011.09.013.
20. Sun H, Zhu J, Ham S. Acoustic evaluation of concrete delaminations using ball-chain impact excitation. J Acoust Soc Am. 2017;141(5):EL477–EL481. https://doi.org/10.1121/1.4983343.
21. Groschup R, Grosse C. MEMS microphone array sensor for air-coupled impact-echo. Sensors. 2015;15(7):14932–14945. https://doi.org/10.3390/s150714932.

AUTHOR BIOGRAPHIES

Johannes F. Scherr, M.Sc., Doctoral Candidate, Chair of Non-Destructive Testing, Technical University of Munich, Franz-Langinger-Straße 10, 81245 Munich, Germany.

Christian U. Grosse, Prof. Dr.- Ing. habil., Chair of Non-Destructive Testing, Technical University of Munich, Franz-Langinger-Straße 10, 81245 Munich, Germany.

How to cite this article: Scherr JF, Grosse CU. Delamination detection on a concrete bridge deck using impact echo scanning. *Structural Concrete*. 2021;22:806–812. https://doi.org/10.1002/suco.202000415